Measurement of the Interfacial Tension of a Phase-Separated Colloid−Polymer Suspension

Els H. A. de Hoog and Henk N. W. Lekkerkerker*

Van't Hoff Laboratory for Physical and Colloid Chemistry, Debye Institute, Utrecht University, Padualaan 8, 3584 CH Utrecht, The Netherlands

Received: January 5, 1999; In Final Form: April 2, 1999

We studied the interfacial tension between coexisting colloid-rich and polymer-rich fluid phases in a phase-separated colloid−polymer mixture. First, the location of the fluid−fluid binodal and the tie lines between the coexisting phases were determined using a recently proposed method that only requires the volumes of the coexisting phases as input. The spinning drop method was used to determine the very low interfacial tension between the coexisting phases. We also used the dynamics of the breakup process of the droplet of one phase suspended in the other to determine the interfacial tension.

1. Introduction

It is well-known that the addition of free nonadsorbing polymers to a colloidal dispersion can induce a phase separation due to the depletion interaction between the colloids. This phenomenon was first theoretically described by Asakura and Oosawa[1] and later by Vrij.[2] The depletion interaction is based on the fact that there is a region around the colloidal particles, the depletion zone, from which the polymers are almost entirely excluded. When the colloidal particles approach each other sufficiently close for the depletion zones to overlap, there is an imbalance in osmotic pressure exerted by the polymers. This imbalance induces an effective attraction between the colloidal particles. The range of the associated depletion potential depends on the size of the polymer; its depth is proportional to the osmotic pressure, which in turn is a function of the concentration of the polymers. Provided the attraction is sufficiently strong, the colloid−polymer suspension phase-separates into a colloid-rich phase and a polymer-rich phase.

Phase transitions in colloid−polymer suspensions have attracted considerable attention, both theoretically and experimentally; see, for example, refs 3−16. It has become clear that for small polymer to colloid size ratios (<0.3) the transition is of the fluid−solid type, while for large size ratios (>0.3) three different phases can occur: two different fluid phases, i.e., a gaslike and a liquidlike phase, and one solid phase, a colloidal crystal. The mechanism and kinetics of these phase transitions have been studied; not only phenomena such as nucleation and growth and spinodal decomposition have been reported[17,18] but also processes of aggregation and gelation.[17,19]

Here, we study the interfacial tension between coexisting phases in a phase-separated colloid−polymer mixture. This quantity is of fundamental interest[20] and plays an important role in phase-separation kinetics[21] and in emulsification processes.[22,23] Nevertheless, so far only a preliminary study[24] is known in which the interfacial tension is measured for just one point in the phase diagram of a phase-separated colloid−polymer mixture. The interfacial tension, or excess free energy per area, is the consequence of a gradual change of the concentration of the colloidal particles and the polymer molecules across the interface between the two coexisting phases. A crude estimate of the interfacial tension γ may be given by the scaling relation $\gamma \propto k_B T\phi/\xi^2$, in which k_B is the Boltzmann constant, T is the temperature, ϕ is the volume fraction of the colloidal particles in the colloid-rich phase, and ξ is a typical length scale related to the interfacial thickness.[25,26] Far from the critical point this interfacial thickness is about the size of the colloid or the polymer correlation length (in the studied system the diameter of the colloids and the polymers are equal). Closer to the critical point this length scale increases, which causes a decrease in the interfacial tension. Although this scaling relation is derived for a single-component system, we expect that it is useful also for more complex systems as a first, crude estimation.

When in the scaling relation the diameter of the particles is inserted for ξ, the interfacial tension of a "gas"−"liquid" type of interface in a demixed colloid−polymer suspension would be in the range of 0.01−0.0001 mN/m. This is an ultralow interfacial tension in comparison with those of atomic gas−liquid interfaces, which are in the range 10−100 mN/m, and also low in comparison with those of purely polymeric systems, i.e., demixed polymer blends and phase-separated polymer solutions, which are known to exhibit low interfacial tensions of a few mN/m. This much lower interfacial tension in colloid−polymer suspensions, even far from the critical point, is caused by the increase of the relevant length scale.

A convenient and accurate method to determine ultralow interfacial tensions between two fluid phases is the spinning drop method,[27,28] which has been used extensively in studies of polymer blends and of microemulsions.[29,30] In this study we apply the spinning drop method (a stationary method) to measure the low interfacial tension between the polymer-rich (low density) and the colloid-rich (high density) coexisting phases in phase-separated colloid−polymer suspensions. In addition we demonstrate that the breakup of a droplet of the low-density phase immersed in the high-density phase provides us with a second method (a dynamical method) to determine the interfacial tension between the two phases, the so-called breaking thread method. This method has been used before in studies of mixtures of highly viscous liquids.[31] The spinning drop setup allows us to establish and analyze the time evolution of the breaking drops.

To determine the interfacial tension from the experimental data obtained by the spinning drop and the breaking thread measurements, the densities and viscosities of the coexisting

* Corresponding author. E-mail: H.N.W.Lekkerkerker@chem.uu.nl.

10.1021/jp990061n CCC: $18.00
Published on Web 06/03/1999

phases are required. The former were obtained by constructing the phase diagram with its tie lines[32] and the latter by means of a constant shear rheometer.

The remainder of this paper is organized as follows: in section 2 the system, the construction of its phase diagram, and the determination of the densities and viscosities of the coexisting phases are described. In section 3 the experimental techniques to determine the interfacial tension are discussed and the results are given. Section 4 gives a discussion of the results, and this paper ends with a conclusion in section 5.

2. Phase Behavior

2.1. System. We studied mixtures of spherical silica colloids and poly(dimethylsiloxane) polymers in the solvent cyclohexane. This system was originally prepared and characterized by Verhaegh in a study of the fluid−fluid transition.[18] The silica colloids are commercially available Ludox spheres (Ludox AS 40%, Dupont) coated with 1-octadecanol (Merck, zur Synthese). The hydrodynamic radius of the particles, obtained by means of dynamic light scattering measurements, is 13 nm with a polydispersity of 19%; the particle density was established at 1.60 g/mL. The polymer we used in our experiments is commercially available poly(dimethylsiloxane) (PDMS, Janssen). The radius of gyration of the polymers was measured by gel permeation chromatography and determined at 14 nm; its molecular weight is 97 000 g/mol ($M_w/M_n = 1.9$), and its density is 0.976 g/mL. The colloid and polymer particles form a stable dispersion in cyclohexane (Baker analyzed). The dispersions are almost transparent because the index of refraction of the particles nearly matches that of cyclohexane. However, the optical contrast turns out sufficiently well to be able to observe clearly the interface between the coexisting fluid−fluid phases.

2.2. Phase Diagram. After homogenization of a colloid−polymer mixture at sufficiently high concentrations of either constituent, the system first becomes turbid, but after a short time the turbidity is reduced and the formation of an interface is observed. Phase separation typically takes place within half an hour to a few hours, depending on the concentrations. The interface is flat and clear. In highly concentrated samples a gel state is found.

Visual inspection of the demixed suspensions along dilution lines (i.e., straight lines through the phase diagram with constant concentration ratio of colloid and polymer) allows one to examine the boundary between the one- and the two-phase regions. However, the construction of tie lines in the phase diagram requires the determination of the composition of the demixed phases. For colloid−polymer mixtures used in this study this is no easy task because standard techniques such as gas chromatography or photospectrometry are not directly applicable. Drying and weighing a known volume of the phase would be an obvious alternative except that the results could be affected by ill-understood drying effects. Recently, however, Bodnár and Oosterbaan[32] proposed a method to construct the tie lines in a phase diagram of a colloidal-gas−colloidal-liquid phase transition, based only on volume measurements of the coexisting phases (along at least three dilution lines) and on the mass balance.

We constructed the phase diagram with the method of Bodnár and Oosterbaan using volume measurements along four dilution lines with polymer-to-colloid concentration ratios of 1.4, 3.9, 7.5, and 21.2. Instead of direct measurements of the volumes of the upper and lower phases, the heights of the two phases in a tube were measured. After the sample tubes were calibrated, the heights were converted to volumes. The volume measurements of the upper and the lower phase were started with a concentrated sample in which no gel state was observed. After each measurement of the volumes, the sample was diluted with a small amount of the solvent cyclohexane, and the procedure was repeated until the sample was so dilute that no phase separation occurred.

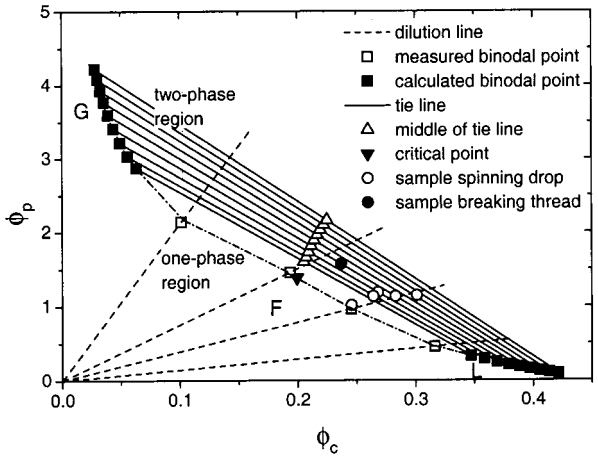

Figure 1. Constructed phase diagram of the colloid−polymer suspension where the polymer volume fraction ϕ_p ($=(N_p/V)(4\pi/3)R_g^3$) is plotted vs the colloid volume fraction ϕ_c. In this diagram are shown the dilution lines (dashed lines), the measured binodal points (open squares), a few of the calculated binodal points (solid squares), a few of the calculated tie lines (straight lines), the middle of the tie lines (up triangles), the critical point (down triangle) estimated by extrapolating the middle of the tie lines to the binodal, the composition of the samples for the spinning drop (open circles), and breaking thread experiments (solid circle). The colloidal-gas, colloidal-liquid, and colloidal-fluid phases are denoted by G, L, and F, respectively.

The phase diagram is shown in Figure 1. Here, the polymer volume fraction ϕ_p is defined as the polymer number density times a spherical volume with radius equal to the radius of gyration of the polymer; this is in fact a volume fraction relative to the crossover value to the semidilute regime. Volume fractions smaller than unity indicate points in the dilute range; volume fractions greater than unity indicate that the solution has entered the entangled semidilute state. The colloid volume fraction ϕ_c is determined by converting the colloid weight fraction using the densities of the colloidal particles and the solvent. The diagram gives the four dilution lines and the measured binodal points on these lines, some of the calculated binodal points, the associated tie lines, and the middle of the tie lines. The binodal points are connected with a dashed line to guide the eye. The colloidal-gas, the colloidal-liquid, and the colloidal-fluid phases are denoted by G, L, and F, respectively. The critical point was estimated by extrapolating the middle of the tie lines to the binodal.

2.3. Densities and Viscosities of the Coexisting Phases. Information on the densities and the viscosities of the coexisting phases is required to analyze the experimental data obtained with the spinning drop and the breaking thread technique.

The densities are determined from the phase diagram. The overall concentrations of the colloids and polymers in a suspension indicate the position in the phase diagram. The tie line through this point in the phase diagram determines the points on the binodal of the two coexisting phases and therefore the concentrations of the colloids and the polymers in both phases. Because the densities of the colloids, the polymers, and the solvent are known, the density of both phases can be calculated. The density differences between the coexisting

TABLE 1: Results of the Five Spinning Drop Experiments[a]

sample	ϕ_c*	ϕ_p*	$\Delta\rho$ [mg/mL]	n	γ [μN/m]
A	0.246	1.016	175	58	3.0 ± 0.7
B	0.264	1.132	240	11	3.8 ± 0.6
C	0.268	1.189	256	7	3.2 ± 0.2
D	0.283	1.133	268	31	4.2 ± 0.4
E	0.301	1.143	291	27	4.5 ± 0.5

[a] For each sample are given the overall volume fraction of colloids, ϕ_c*, and polymers, ϕ_p*, the density difference between the coexisting phases, $\Delta\rho$, the number of analyzed droplets, n, and the determined interfacial tension, γ

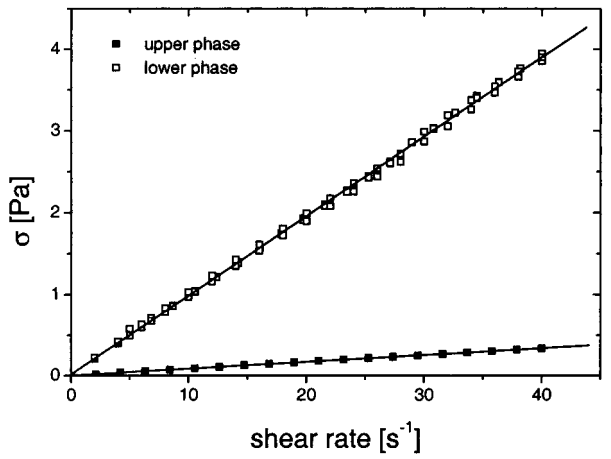

Figure 2. Stress σ as a function of the shear rate for the upper and the lower phase. The slope of the graphs is the shear viscosity.

phases in the suspensions used in the spinning drop technique are given in Table 1 and are in the range of 150−300 mg/mL.

The viscosities of the two coexisting phases of the sample used in the breaking thread experiment were measured with a Contraves LS40 rheometer with a Couette geometry (DIN 406) equipped with a vapor lock filled with cyclohexane. The temperature within the rheometer was kept at 20 °C by a thermostatic bath that circulated water around the measuring geometry. The shear rates were varied between 0 and 40 s^{-1}. The upper and lower phases were each measured twice. The measured stress σ versus shear rate is given in Figure 2. The slope of the linear fit gives the viscosity. The lower phase has a viscosity of 97.1 mPa s, and the viscosity of the upper phase is 8.4 mPa s. Because it is possible to fit the data linearly, we conclude that both phases behave as Newtonian liquids.

3. Interfacial Tension

3.1. Spinning Drop Method. *Principle.* The spinning drop technique is based on the fact that the elongation of the droplet due to centrifugal forces is balanced by the interfacial tension between the two phases.

Consider a tube filled with the high-density phase and a droplet of the low-density phase. The tube rotates around a horizontal axis at a certain rotational speed ω (see Figure 3). From the measurement of the length L and diameter D of the droplet, the interfacial tension can be calculated using an equation derived by Princen et al.:[28]

$$\gamma = \frac{\omega^2 a^3 \Delta\rho}{2\alpha} \tag{1}$$

Here, a is the curvature of the top of the drop and α is a dimensionless number, both of which are determined by L and D.[28]

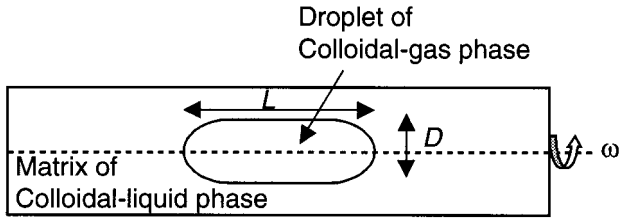

Figure 3. Spinning drop tube filled with the two phases. The system is rotating around its axis with a rotational speed ω. For clearness' sake the droplet is drawn much too large for this scale.

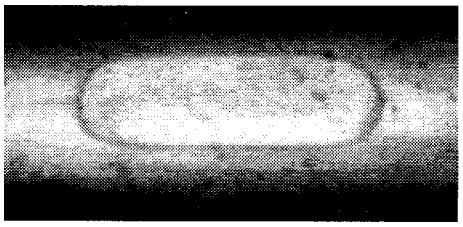

Figure 4. Photograph of a droplet of the low-density phase immersed in the high-density phase of a demixed colloid−polymer suspension rotating at a rotational speed of 60 rad/s.

Experiment. A home-built spinning drop tensiometer was used.[33] The internal diameter of the spinning drop tube measures 4 mm and its length 4 cm. The dense phase was injected with a glass capillary, and the tube was closed with a Teflon stopper on each side; one of the stoppers had a hole through which the lower density phase was injected with a microsyringe. This hole could be closed with a small screw. A droplet of the lower density phase was formed by rotating the tube around its axis horizontally. When the rotational speed is decreased, the drop breaks up into several smaller droplets. The length and the diameter of the droplets were measured with a crosswire on the microscope and using a micrometer. The rotational speed was measured with an optical sensor. For these measurements we choose the rotational speeds in the range of $35 < \omega < 105$ rad/s; the temperature was fixed at 20 °C.

The interfacial tension was determined for five points in the two-phase region in the phase diagram (see Figure 1). The five samples were chosen in such a way that they had a relatively large volume of the high-density phase, which was convenient in the experiments. To obtain the interfacial tension of each sample, the length and diameter of many droplets were measured many times, at two or three different moments in time. A correction factor accounting for the curvature of the tube was used in establishing the diameter of the droplets.[34]

Although the technique is straightforward in principle, a number of difficulties were encountered. First, the solvent evaporated very quickly, before an equilibrium was reached. A more effectively sealing method making use of the small screw in the Teflon stopper was used. The evaporation within the measuring time was now negligible. Second, the tube filling procedure is difficult because of the small amounts of the phases ($\sim$1 μL of low-density phase and $\sim$1 mL of high-density phase) and the need to avoid air bubbles in the tube. Third, the optical contrast of the boundaries of the droplet was low because of the small difference in the index of refraction between the two phases ($\Delta n \approx 0.005$). Attachment of a CCD camera to the setup made the method more convenient.

Results. A CCD photograph of a typical droplet is shown in Figure 4. The interfacial tension γ was determined with eq 1 from the measurements of the length and diameter of the droplets. The results are given in Table 1; data of the overall volume fraction of colloids ϕ_c* and polymers ϕ_p*, the density

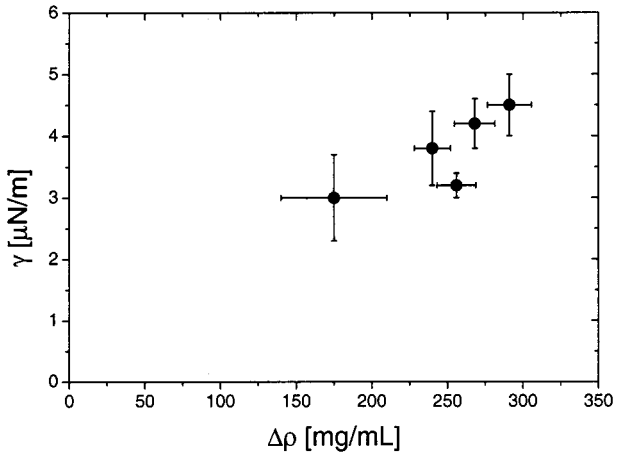

Figure 5. Interfacial tension as a function of the density difference between the two phases as measured with the spinning drop method.

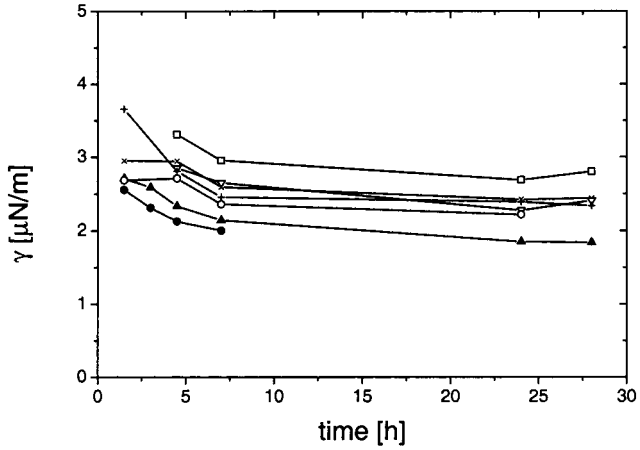

Figure 6. Interfacial tension as a function of time for several different droplets of sample A. The points for a single droplet are connected with a solid line.

difference $\Delta\rho$, and the number of determined droplets n of each sample are included in this table. The density difference was determined as described in section 2.3. In the case of sample A the point in the phase diagram did not fit on a calcultated tie line, and therefore, an approximate tie line was drawn through the point with a slope extrapolated from the slopes of the calculated tie lines in the two-phase region. The determined interfacial tension ranges from 0.0030 to 0.0045 mN/m. If we plot the interfacial tension as a function of the density difference (see Figure 5), a decrease of interfacial tension with a decrease of density difference is found. The density difference between the two phases is used here as a parameter for the location of the different samples in the phase diagram relative to the critical point. A long equilibration time of approximately 10 h is shown in Figure 6, where the interfacial tension is given as a function of time. Here, time zero denotes the time at which the droplet was formed by breaking up a larger drop. Such a long equilibration time in spinning drop experiments has been reported before.[29,35]

3.2. Breaking Thread Method. *Principle.* In the breaking thread method the interfacial tension can be estimated by following the initial stage in time of the breakup of an elongated drop into smaller droplets.

Already in 1878, Rayleigh[36] treated the instability of a long, thin, cylindrical liquid thread, and this work was extended by Tomotika[37] in 1935. Later, Rumscheidt and Mason[31] realized that this theory could be used for determination of the interfacial

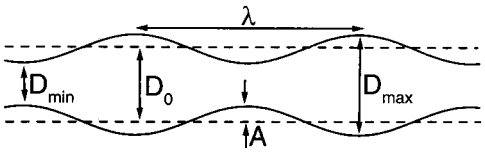

Figure 7. Simplified representation of sinusoidal disturbances on the elongated drop. λ is the wavelength of the disturbance, A the amplitude, D_0 the original diameter, D_{min} and D_{max} the minimum and the maximum diameter.

tension. This method is also referred to as the breaking thread method, and it has been applied to, for example, oils[38] and polymers.[21,38]

Consider a long liquid cylinder with radius R and viscosity η_1 surrounded by another liquid with viscosity η_2.[21] Initially, the elongated drop exhibits only small sinusoidal disturbances (see Figure 7). The disturbances with a wavelength λ larger than the original circumference of the drop, $\lambda \geq 2\pi R$, will grow and eventually cause the drop to break. The amplitude A of the disturbance grows exponentially with time t. The fastest growing wavelength with growth rate q_m will be dominant. A relation for the interfacial tension as a function of this growth rate is given by[21]

$$\gamma = \frac{\eta_2 D_0 q_m}{\Omega_m} \tag{2}$$

Here, D_0 is the initial diameter of the droplet and Ω_m is given by[21] $\Omega_m = (1 - (\pi D_0/\lambda)^2)f$, with f a function of $\pi D_0/\lambda$ and η_1/η_2. The growth rate q_m follows from $\ln(A(t)/R) \propto q_m t$,[21] and it can be determined from a plot of $\ln(A(t)/R)$ versus time t. Here, $A(t)$ is the amplitude as a function of the time.

Experiment. We used the spinning drop setup to measure the evolution of a breaking drop in time. The breaking of a droplet was achieved by a sudden decrease of an initial rotational speed ω_i to a final rotational speed ω_f (e.g., $\omega_i = 600$ rad/s and $\omega_f = 60$ rad/s). The breakup process was monitored by taking pictures with a CCD camera at fixed time intervals. The CCD camera was attached to the spinning drop setup, and its performance was checked by comparing the results of measurements of the length and diameter of several droplets in equilibrium, using both the camera and the microscope. The data coincide within an experimental error of 3%. The digital pictures taken by the CCD camera were analyzed by computer with an imaging program.

A sample with a colloid volume fraction of 0.237 and a polymer volume fraction of 1.571 was used (see Figure 1). Two experiments were done with two different final rotational speeds, the first with $\omega_f = 50$ rad/s and the second with $\omega_f = 60$ rad/s. In both experiments the diameter of the drop as a function of time was measured at four different positions along the elongated drop, two at a minimum and two at a maximum.

Results. Photographs of different stages of a breakup process are shown in Figure 8. Note the presence of a very small droplet between the first and the second drop. The formation of such satellite droplets in other suspensions has been reported before.[40] Figure 9 gives magnified pictures of an observed satellite formation.

The interfacial tension was determined with eq 2 in two experiments with different final rotational speed. In the first experiment the interfacial tension of 0.0025 mN/m is found, and in the second experiment with a higher final rotational speed an interfacial tension of 0.0014 mN/m is found (see Table 2).

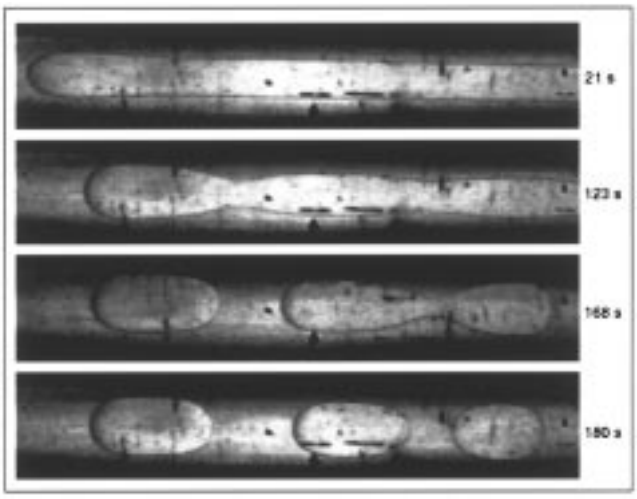

Figure 8. Breakup of an elongated droplet. Only part of the long droplet is shown. In about 3 min the droplet has broken up into smaller droplets. Between the small droplets a very small droplet has formed, which can hardly be seen in this picture.

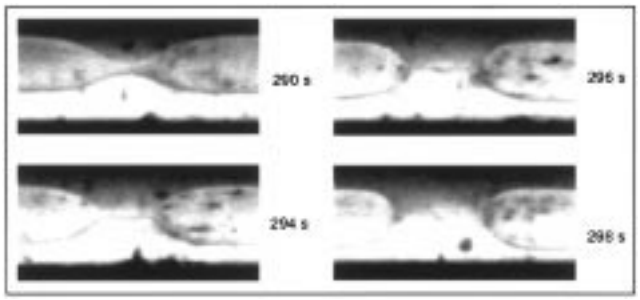

Figure 9. Detail of photographs of a breakup process in which the satellite formation is shown.

TABLE 2: Results of the Two Breaking Thread Experiments[a]

	experiment 1	experiment 2
q_m [s^{-1}]	0.02411	0.01333
D_0 [mm]	0.266	0.275
η_2 [mPa s]	97.1	97.1
Ω_m	0.25	0.25
ω_f [rad/s]	50	60
γ [μN/m]	2.5	1.4

[a] For each experiment are given the growth rate, q_m, the original diameter, D_0, the viscosity of the high-density phase, η_2, the value of Ω_m,[21] the final rotational speed, ω_f, and the measured interfacial tension, γ

4. Discussion

The results of the interfacial tension measurements reported are in good agreement with the scaling relation $\gamma \propto k_B T\phi/\xi^2$. By use of ξ, the diameter of the colloids (see Introduction), this scaling relation predicts an interfacial tension in the range 0.01−0.0001 mN/m. Although our results are in the same order of magnitude as those of Vliegenthart and Lekkerkerker,[24] they are in fact about 3 times lower. This can partly be explained by a less accurate determination of the density difference in ref 24 and the fact that the equilibration time in their experiments, limited by the evaporation of the solvent, was much shorter. From Figure 6 we can see that this could lead to a higher measured interfacial tension.

From Figure 5 we see that closer to the critical point (smaller density difference) the interfacial tension becomes smaller. The decrease of the interfacial tension can be understood in terms of a more diffuse interface and a better miscibility of the two phases; i.e., the concentration difference of the components between the two phases decreases.

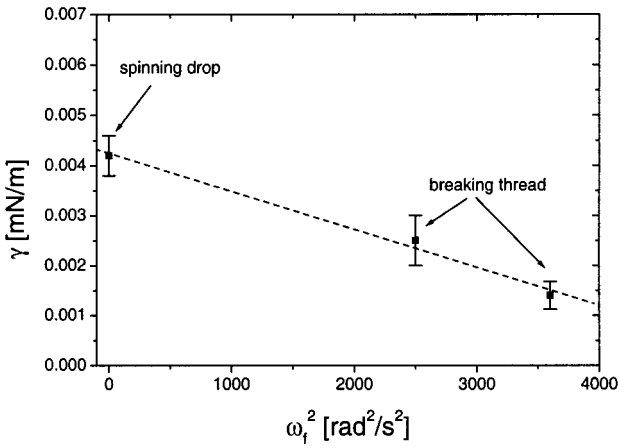

Figure 10. Interfacial tension as a function of the squared final rotational speed as determined by the breaking thread method. The value given at a zero rotational speed was measured with the spinning drop method in a sample (sample D) with the same density difference as the sample used in the breaking thread experiments.

The small but significant difference between the interfacial tensions determined with the spinning drop method and with the breaking thread method can perhaps be explained by the fact that in the breaking thread experiments a nonnegligible centrifugal force is present in the final state in order to prevent the droplets from sedimenting. The growth rate of the distortions, and hence the interfacial tension calculated with eq 2, will be influenced by this centrifugal force. Since this effect will be an even function of the final rotational speed, we have plotted in Figure 10 the calculated interfacial tension versus the square of the final rotational speed. Assuming that for sufficiently small final rotational speeds such a plot is a straight line, we can extrapolate to zero final rotational speed. The value of the interfacial tension determined in this way is in good agreement with the value obtained by the spinning drop method.

5. Conclusion

In this study we reported on the measurement of the interfacial tension of demixed colloid−polymer suspensions using the spinning drop method as well as the breaking thread method. The fluid−fluid binodal of the system was determined, and the tie lines in the phase diagram were constructed using a method based on volume measurements of the coexisting phases. From this phase diagram the location of the used samples and the densities of the coexisting phases needed for the analysis of the spinning drop experiments could be obtained accurately. With the spinning drop method interfacial tensions in the range 0.0030−0.0045 mN/m were found; the interfacial tension increases with an increasing density difference between the coexisting phases. Furthermore, we demonstrated that the breaking thread method is a useful method to determine the interfacial tension in colloid−polymer suspensions. Extrapolation of the interfacial tension, measured with the breaking thread method, to zero final rotational speed yields an interfacial tension that is in agreement with spinning drop results.

Acknowledgment. We thank Gerrit Vliegenthart, Jan Dhont, and Paul van der Schoot for fruitful discussions, Nynke Verhaegh for supplying us with the colloid particles, Bonny Kuipers for help with the optical configuration, and Martijn de

Groot for writing a computer imaging program for the analysis of the CCD photographs. This work was supported by the Stichting voor Fundamenteel Onderzoek der Materie (Foundation for Fundamental Research on Matter), which is part of the Nederlandse Organisatie voor Wetenschappelijk Onderzoek (Netherlands Organization for the Advancement of Research).

References and Notes

(1) Asakura, S.; Oosawa, F. *J. Chem. Phys.* **1954**, *22*, 1255.
(2) Vrij, A. *Pure Appl. Chem.* **1976**, *48*, 471.
(3) Sieglaff, C. *J. Polym. Sci.* **1959**, *41*, 319.
(4) Cowell, C.; Lin-In-On, R.; Vincent, B. *J. Chem. Soc., Faraday Trans. 1* **1978**, *74*, 337.
(5) de Hek, H.; Vrij, A. *J. Colloid Interface Sci.* **1979**, *70*, 592.
(6) Joanny, J. F.; Leibler, L.; de Gennes, P. G. *J. Polym. Sci., Polym. Phys. Ed.* **1979**, *17*, 1073.
(7) Gast, A. P.; Hall, C. K.; Russel, W. B. *J. Colloid Interface Sci.* **1983**, *96*, 251.
(8) Sperry, P. R. *J. Colloid Interface Sci.* **1984**, *99*, 97.
(9) Leal Calderon, F.; Bibette, J.; Bias, J. *Europhys. Lett.* **1993**, *23*, 653.
(10) Lekkerkerker, H. N. W.; Poon, W. C. K.; Pusey, P. N.; Stroobants, A.; Warren, P. B. *Europhys. Lett.* **1992**, *20*, 559.
(11) Pusey, P. N.; Pirie, A. D.; Poon, W. C. K. *Physica A* **1993**, *201*, 322.
(12) Meijer, E. J.; Frenkel, D. *J. Chem. Phys.* **1994**, *100*, 6273.
(13) Ilett, S. M.; Orrock, A.; Poon, W. C. K.; Pusey, P. N. *Phys. Rev. E* **1995**, *51*, 1344.
(14) Schaink, H. M.; Smit, J. A. M. *J. Chem. Phys.* **1997**, *107*, 1004.
(15) Verma, R.; Crocker, J. C.; Lubensky, T. C.; Yodh, A. G. *Phys. Rev. Lett.* **1998**, *81*, 4004.
(16) Vincent, B.; Edwards, J.; Emmett, S.; Croot, R. *Colloids Surf.* **1988**, *31*, 267.
(17) Poon, W. C. K.; Pirie, A. D.; Pusey, P. N. *Faraday Discuss.* **1995**, *101*, 65.
(18) Verhaegh, N. A. M.; van Duijneveldt, J. S.; Dhont, J. K. G.; Lekkerkerker, H. N. W. *Physica A* **1996**, *230*, 409.
(19) Verhaegh, N. A. M.; Asnaghi, D.; Cipelletti, L. *Physica A* **1997**, *242*, 104.
(20) Vrij, A. *Physica A* **1997**, *235*, 120.
(21) Elemans, P. H. M.; Janssen, J. M. H.; Meijer, H. E. H. *J. Rheol.* **1990**, *34*, 1311.
(22) Siggia, E. D. *Phys. Rev. A* **1979**, *20*, 595.
(23) Syrbe, A.; Fernandes, P. B.; Dannenberg, F.; Bauer, W.; Klostermeyer, H. In *Food macromolecules and colloids*; Dickenson, E., Lorient, D., Eds.; Royal Society of Chemistry Special Publications: Cambridge, 1995; Vol. 156, pp 328−339.
(24) Vliegenthart, G. A.; Lekkerkerker, H. N. W. *Prog. Colloid Polym. Sci.* **1997**, *105*, 27.
(25) Rowlinson, J. S.; Widom, B. *Molecular theory of capillarity*; Clarendon Press: Oxford, 1982.
(26) de Gennes, P. G. *Scaling concepts in polymer physics*; Cornell University Press: Ithaca, NY, 1979.
(27) Vonnegut, B. *Rev. Sci. Instrum.* **1942**, *13*, 6.
(28) Princen, H. M.; Zia, I. Y. Z.; Mason, S. G. *J. Colloid Interface Sci.* **1967**, *23*, 99.
(29) Patterson, H. T.; Hu, K. H.; Grindstaff, T. H. *J. Polym. Sci., Part C* **1971**, *34*, 31.
(30) Kegel, W. K.; van Aken, G. A.; Bouts, M. N.; Lekkerkerker, H. N. W.; Overbeek, J. Th. G.; de Bruyn, P. L. *Langmuir* **1993**, *9*, 252.
(31) Rumscheidt, F. D.; Mason, S. G. *J. Colloid Sci.* **1962**, *17*, 260.
(32) Bodnár, I.; Oosterbaan, W. D. *J. Chem. Phys.* **1997**, *106*, 7777.
(33) van Aken, G. A. Ph.D. Thesis, Utrecht University, Utrecht, The Netherlands, 1990.
(34) Coucoulas, L. M.; Dawe, R. A.; Mahers, E. G. *J. Colloid Interface Sci.* **1983**, *93*, 281.
(35) Manning, C. D.; Scriven, L. E. *Rev. Sci. Instrum.* **1977**, *48*, 1699.
(36) Lord Rayleigh, *Proc. London Math. Soc.* **1878**, *10*, 4.
(37) Tomotika, S. *Proc. R. Soc., Ser. A* **1935**, *150*, 322.
(38) Tjahjadi, M.; Ottino, J. M.; Stone, H. A. *AIChE J.* **1994**, *40*, 385.
(39) Carriere, C. J.; Cohen, A.; Arends, C. B. *J. Rheol.* **1989**, *33*, 681.
(40) Tjahjadi, M.; Stone, H. A.; Ottino, J. M. *J. Fluid Mech.* **1992**, *243*, 297.